Front. Phys. 11(3), 110301 (2016)
DOI 10.1007/s11467-015-0530-9

RESEARCH ARTICLE

Dynamic fragmentation in a quenched two-mode Bose–Einstein condensate

Shu-Yuan Wu (吴淑媛)[1,2], **Hong-Hua Zhong** (钟宏华)[1,2,3], **Jia-Hao Huang** (黄嘉豪)[1,2], **Xi-Zhou Qin** (秦锡洲)[1,2], **Chao-Hong Lee** (李朝红)[1,2,†]

[1] *School of Physics and Astronomy, Sun Yat-Sen University, Guangzhou 510275, China*

[2] *State Key Laboratory of Optoelectronic Materials and Technologies, Sun Yat-Sen University, Guangzhou 510275, China*

[3] *Department of Physics, Jishou University, Jishou 416000, China*

Corresponding author. E-mail: [†] *chleecn@gmail.com*

Received September 10, 2015; accepted October 14, 2015

We investigate the fragmentation in a two-mode Bose–Einstein condensate with Josephson coupling. We explore how the fragmentation and entropy of the ground state depend on the intermode asymmetry and interparticle interactions. Owing to the interplay between the asymmetry and the interactions, a sequence of notches and plateaus in the fragmentation appears with the single-atom tunneling and interaction blockade, respectively. We then analyze the dynamical properties of the fragmentation in three typical quenches of the asymmetry: linear, sudden, and periodic quenches. In a linear quench, the final state is a fragmented state due to the sequential Landau–Zener tunneling, which can be analytically explained by applying the two-level Landau–Zener formula for each avoided level crossing. In a sudden quench, the fragmentation exhibits persistent fluctuations that sensitively depend on the interparticle interactions and intermode coupling. In a periodic quench, the fragmentation is modulated by the periodic driving, and a suitable modulation may allow one to control the fragmentation.

Keywords fragmentation, two-mode BEC, quantum quench

PACS numbers 03.75.Hh, 67.85.De, 03.75.Lm

1 Introduction

In 1956, Penrose and Onsager [1] gave the concept of Bose–Einstein condensation (BEC) based on the single-particle density matrix (SPDM) for an interacting system of N particles. Correspondingly, the eigenvalues and eigenvectors are referred to as the occupation numbers and natural orbitals, respectively. Simple BEC appears when the SPDM has only one macroscopic eigenvalue of order N. However, the system is said to be fragmented if the SPDM has two or more eigenvalues of order N, i.e., there is more than one macroscopically occupied state. Moreover, the system is strongly correlated if all eigenvalues are of order 1, and there is no trace of condensation [2]. Ground-state fragmentation has been observed in several systems involving specific spatial or spin symmetries. Examples include scalar bosons in either a single-trap [3, 4] or a double-trap potential [5], attractive condensates in a one-dimensional ring trap [6], two-component Bose gases [7], and spinor Bose gases [8–13].

A typical system for exploring the mechanism of fragmentation is a two-mode Bose–Josephson junction (BJJ) [2, 14], which can be realized by loading Bose condensed atoms into a double-well potential. Usually, strong interparticle interactions will induce a high degree of fragmentation [15–17], and different kinds of interactions will cause different types of fluctuations. As pointed out in [18], both repulsive and attractive interactions can lead to fragmented ground states; however, they have completely different two-particle correlations. In the case of repulsive interactions, the ground state is a Fock state with the number fluctuations $(\Delta\hat{N})^2 \sim 0$, which is clearly fragmented. In the case of attractive interactions, the ground state is a general Schrödinger-cat-like state and "superfragmented", as the number fluctuations $(\Delta\hat{N})^2$ is huge, i.e., of order N^2 [9]. In addition, the ground state is found to be a pair condensate, which is also fragmented, in the presence of strong pair tunneling [19]. The ground-state fragmentation in a BJJ

has been extensively studied by employing the Bose–Hubbard dimer. In the case of weak interactions, dynamic fragmentation has been uncovered [20]. However, the out-of-equilibrium behaviors of fragmentation, such as the dynamic fragmentation in quenched systems, have rarely been studied.

A quench refers to varying a physical parameter in order to drive the system across a quantum phase transition. The nonadiabatic dynamics of isolated quantum systems following a quantum quench have attracted great interest in both experiments [21–25] and theories [26–37]. Owing to the well-developed techniques for tuning physical parameters (including the on-site energy, the interaction energy, the tunneling strength, etc.), the out-of-equilibrium dynamics such as thermalization [38–43], the dynamics of a quantum phase transition [44–48], and quantum transport [49–52] in quenched many-body quantum systems have been extensively investigated.

In this article, we have investigated the fragmentation of a coupled two-mode Bose–Einstein condensate, which undergoes quantum quenches. First, we show how the ground-state fragmentation and entropy depend on the asymmetry and interactions. Interestingly, sequential fragmentation appears with the sequential interaction blockade owing to the interplay between the asymmetry and the interparticle interactions. Further, we discuss the fragmentation dynamics following three typical quenches of the asymmetry: linear, sudden, and periodic. The linear quench is actually a many-body Landau–Zener (LZ) process in which nonadiabatic transitions take place when the asymmetry is driven across the anticrossing points. Below, we will discuss how these nonadiabatic transitions affect the fragmentation. Another crucial question to be answered is the robustness of fragmentation against an instantaneous perturbation, the so-called sudden quench. Regarding periodic driving, we demonstrate that the system can be approximated by an undriven system with a renormalized tunneling strength if the driving frequency is sufficiently high. The renormalization of the tunneling strength via periodic driving provides an efficient method to modulate the fragmentation.

The structure of this article is as follows. In Section 2 we describe our model. In Section 3, we define the measure of the degree of fragmentation and investigate the ground-state fragmentation and entropy. We explore how the ground-state fragmentation and entropy depend on the asymmetry and interactions. In Section 4, we address dynamic fragmentation following three typical quantum quenches. In the last section, we summarize our results.

2 Model

We consider the system of Bose condensed atoms in a double-well potential. If the barrier between the two wells is sufficiently high, one can apply the two-mode approximation, such that the system can be described by the two-mode Bose–Hubbard Hamiltonian [53–62]:

$$\hat{H} = \frac{\delta}{2}(\hat{n}_2-\hat{n}_1)+\frac{E_c}{8}(\hat{n}_2-\hat{n}_1)^2-T(\hat{a}_1^\dagger\hat{a}_2+\hat{a}_1\hat{a}_2^\dagger), \tag{1}$$

where $\hat{a}_i^\dagger$, $\hat{a}_i$, and $\hat{n}_i=\hat{a}_i^\dagger\hat{a}_i$ are the creation, annihilation, and number operators, respectively. Here, δ denotes the asymmetry between the two wells, E_c is the on-site interaction energy, and T is the interwell tunneling strength. It is apparent that the Hamiltonian conserves the total number of atoms $N=\langle\hat{N}\rangle=\langle\hat{n}_1+\hat{n}_2\rangle$, as $[\hat{N},\hat{H}]=0$. By applying the Wigner–Schwinger pseudospin representation [63] $\hat{J}_x=\frac{1}{2}(\hat{a}_2^\dagger\hat{a}_1+\hat{a}_1^\dagger\hat{a}_2)$, $\hat{J}_y=\frac{1}{2\mathrm{i}}(\hat{a}_2^\dagger\hat{a}_1-\hat{a}_1^\dagger\hat{a}_2)$, $\hat{J}_z=\frac{1}{2}(\hat{a}_2^\dagger\hat{a}_2-\hat{a}_1^\dagger\hat{a}_1)$, the Hamiltonian is equivalent to the giant spin model:

$$\hat{H}=\delta\hat{J}_z+\frac{E_c}{2}\hat{J}_z^2-2T\hat{J}_x. \tag{2}$$

The above Hamiltonian can be diagonalized in the $(N+1)$-dimensional space spanned by the basis $|J=N/2,J_z=m\rangle$ with $m=-N/2,-N/2+1,\ldots,N/2$. Thus, an arbitrary state can be written in form of [57]

$$|\Psi\rangle=\sum_m C_m|\frac{N}{2},m\rangle, \tag{3}$$

where the complex number C_m denotes the probability amplitude of the state $|N/2,m\rangle$.

Here, we only consider the case of repulsive interactions (i.e., $E_c>0$). The system can be separated into three different regimes by the ratio of E_J/E_c, where $E_J=NT$ is the junction energy [2, 64]: the Rabi regime ($E_J/E_c\gg N^2$), the Josephson regime ($1\ll E_J/E_c\ll N^2$), and the Fock regime ($E_J/E_c\ll 1$). In the Rabi regime, the ground state is an $SU(2)$ coherent state, and the system possesses no fragmentation. In the Josephson and Fock regimes, the coherent state can be turned into a Schrödinger-cat-like state, which is fragmented, as the number fluctuations are reduced [17]. In Fig. 1, we show the energy spectra for different values of E_J/E_c. If E_c between the particles dominates the Hamiltonian, the ground state undergoes N avoided level crossings, which correspond to transferring one particle from one well to the other. As the tunneling strength increases, the avoided level crossings open and develop a swallowtail-like loop structure in the excited states.

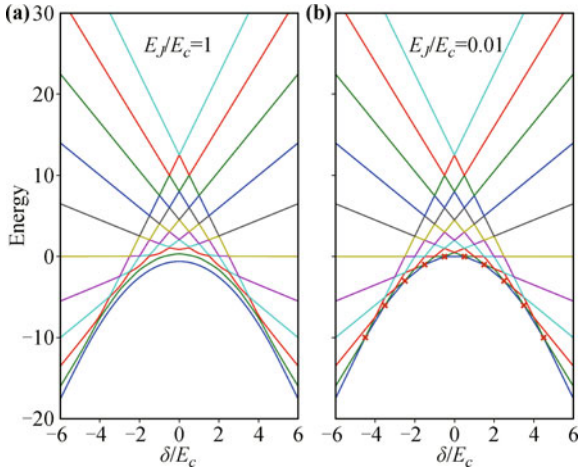

Fig. 1 The energy spectra of the Hamiltonian in Eq. (2) versus δ/E_c for **(a)** $E_J/E_c = 1$ and **(b)** $E_J/E_c = 0.01$. Red crosses denote the avoided level crossings. Here, the total number of atoms is $N = 10$.

3 Fragmentation and entropy of ground states

To understand the dynamics of fragmentation in quantum quenches, we analyze the fragmentation of the instantaneous ground states at first. Below, we will show how the ground-state fragmentation depends on the asymmetry and interactions and also briefly discuss the corresponding entropies.

3.1 Fragmentation

The general concept of BEC is defined by using the SPDM $\rho^{(1)}$ [1]:

$$\rho^{(1)}_{\boldsymbol{r},\boldsymbol{r'}} = \langle \hat{\psi}^\dagger(\boldsymbol{r'})\hat{\psi}(\boldsymbol{r})\rangle, \tag{4}$$

where $\hat{\psi}^\dagger(\boldsymbol{r})$ and $\hat{\psi}(\boldsymbol{r})$ are the bosonic field operators, and $\langle \ldots \rangle$ denotes the average. Following this definition, $\rho^{(1)}$ is a Hermitian matrix with real eigenvalues. Therefore, one can write the SPDM in the form of

$$\rho^{(1)}_{\boldsymbol{r},\boldsymbol{r'}} = \sum_i \phi(\boldsymbol{r'})^* \lambda_i \phi(\boldsymbol{r}), \tag{5}$$

where λ_i denotes the eigenvalues, and $\phi(\boldsymbol{r})$ denotes the corresponding orthonormal eigenfunctions [2, 17].

To characterize the degree of condensation, one has to diagonalize $\rho^{(1)}$ and analyze its eigenvalues. For a given state $|\psi\rangle$, we have

$$\rho^{(1)}_{\mu,\nu} = \langle \psi | \hat{a}^\dagger_\mu \hat{a}_\nu | \psi \rangle. \tag{6}$$

The appearance of fragmentation corresponds to the emergence of more than one macroscopic eigenvalue of the SPDM, which means particles occupying more than one state/orbit. To characterize the fragmentation, one can use the relative occupation n_0/N, where n_0 denotes the maximum occupation number [5, 20]. Here, for our system, it is convenient to define the degree of fragmentation as

$$F = \frac{2(N - \lambda_{\max})}{N}, \tag{7}$$

where $\lambda_{\max}$ is the maximum eigenvalue of $\rho^{(1)}$.

F has a minimum of 0 in the strong asymmetry limit, where the SPDM has a single macroscopic eigenvalue $\lambda_{\max} = N$, leading to all atoms condensed in a single-particle orbit; thus, the system is a pure Bose–Einstein condensate. The maximum of F is 1 in the limit of strong interactions, where the two modes are equally occupied with $\lambda_{\max} = N/2$, and the system is fully fragmented [17]. A transition from a zero F to a nonzero F indicates the occurrence of fragmentation.

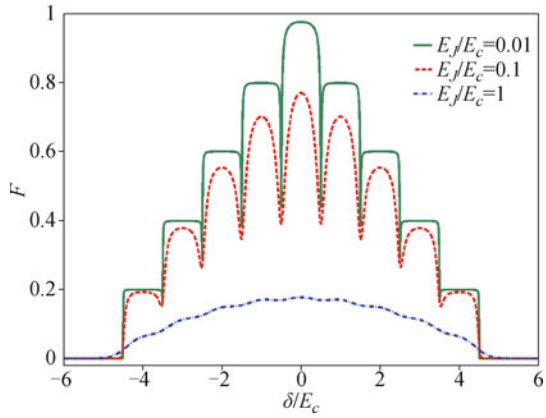

Fig. 2 The degree of ground-state fragmentation F versus δ/E_c and different values of E_J/E_c. The blue dash-dotted, red dashed, and green solid lines correspond to $E_J/E_c = 1$, 0.1, and 0.01, respectively. Here, the total number of atoms is $N = 10$.

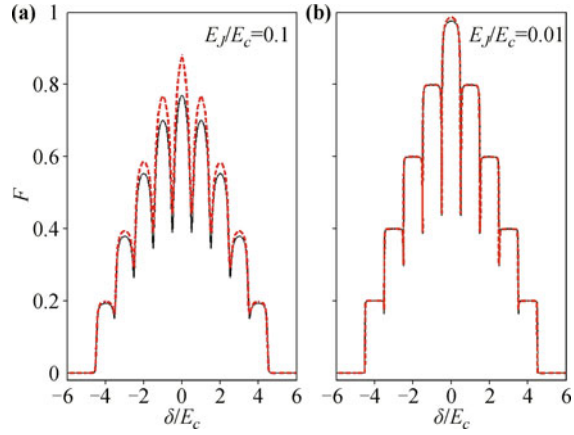

Fig. 3 A comparison of the perturbation (*red dashed lines*) and numerical (*solid lines*) results for **(a)** $E_J/E_c = 0.1$ and **(b)** $E_J/E_c = 0.01$.

In Fig. 2, we show how the ground-state fragmentation depends on the scaled asymmetry δ/E_c. The asymmetry prefers all atoms to be located in the lower well, whereas the repulsive interactions prefer equal atomic populations in the two wells. If the asymmetry dominates, almost all of the atoms are located in one well; therefore, the system does not exhibit fragmentation. As $|\delta/E_c|$ decreases, the interactions begin to dominate, atoms tunnel between two wells to seek the state of zero population difference, and fragmentation appears. The system reaches the maximum degree of fragmentation at $\delta/E_c = 0$.

It can be seen that the fragmentation is more significant for smaller values of E_J/E_c, which correspond to stronger interactions. Before the asymmetry begins to dominate, the ground-state properties depend on E_J/E_c. For large E_J/E_c, atoms are delocalized, and the system is globally phase coherent [65], possessing no fragmentation. As the interactions become stronger, the number fluctuations in each well are squeezed, and the ground state is then localized in a few atom number states, which brings about an increase in the fragmentation [17, 64].

In the Fock regime ($E_J/E_c \ll 1$), the system exhibits a series of fragmentation notches and plateaus by varying the asymmetry δ. Neglecting the tunneling term, the energy for the eigenstate with a quasiangular momentum m is given as $E(m) = \delta m + \frac{E_c}{2}m^2$, and two eigenstates become degenerate when $E(m) = E(m+1)$. At the critical points of $\delta = -(m+\frac{1}{2})E_c$ for $m = -\frac{N}{2}, -\frac{N}{2}+1, \ldots, \frac{N}{2}-1$, single-atom resonant tunneling takes place, and fragmentation notches appear owing to the balance between the interactions and the asymmetry [66]. Between fragmentation notches, fragmentation plateaus corresponding to the interaction blockade appear.

One can also employ a perturbation analysis to analyze the ground-state fragmentation. The ground state can be expressed as $|\Psi\rangle = \beta_1|\psi_1\rangle + \beta_2|\psi_2\rangle$, where $|\psi_1\rangle = |\frac{N}{2}, m\rangle$ and $|\psi_2\rangle = |\frac{N}{2}, m'\rangle$ are the two lowest states, $m' = m-1$ for $\delta < 0$, and $m' = m+1$ for $\delta > 0$. The two coefficients $\{\beta_1, \beta_2\}$ are determined by the eigenvalue problem

$$\begin{pmatrix} H_{11} & H_{12} \\ H_{21} & H_{22} \end{pmatrix} \begin{pmatrix} \beta_1 \\ \beta_2 \end{pmatrix} = E \begin{pmatrix} \beta_1 \\ \beta_2 \end{pmatrix}, \tag{8}$$

where $H_{ij} = \langle\psi_i|\hat{H}|\psi_j\rangle (i,j = 1,2)$ [66]. For simplicity, we assume $\delta < 0$ for the following discussion, but the derivation can also be extended to $\delta > 0$. Near the critical points, we can write δ as $\delta = \delta_m + \xi$, where $|\xi| \leqslant \frac{E_c}{2}$. After some calculations, we have

$$\begin{aligned} \beta_1 &= -\frac{1}{\Theta}\frac{\xi - \sqrt{T^2(N+2m)(N-2m+2)+\xi^2}}{T\sqrt{(N+2m)(N-2m+2)}}, \\ \beta_2 &= \frac{1}{\Theta}, \\ \Theta^2 &= \frac{2\xi^2 + 2T^2(N+2m)(N-2m+2)}{T^2(N+m)(N-2m+2)} \\ &\quad - \frac{2\xi\sqrt{T^2(N+2m)(N-2m+2)}}{T^2(N+m)(N-2m+2)}, \end{aligned} \tag{9}$$

where Θ^2 is the normalization factor. For $\xi = 0$, this leads to $\beta_1 = \beta_2 = 1/\sqrt{2}$; that is, the ground state is the equal-probability superposition of $|\psi_1\rangle$ and $|\psi_2\rangle$. The corresponding SPDM can be written as

$$\rho^{(1)} = \begin{pmatrix} \rho_{11}^{(1)} & \rho_{12}^{(1)} \\ \rho_{21}^{(1)} & \rho_{22}^{(1)} \end{pmatrix}, \tag{10}$$

where the four elements are

$$\begin{aligned} \rho_{11}^{(1)} &= \frac{N}{2} - m + \gamma, \\ \rho_{12}^{(1)} &= \rho_{21}^{(1)} = \eta, \\ \rho_{22}^{(1)} &= \frac{N}{2} + m - \gamma, \end{aligned} \tag{11}$$

where

$$\begin{aligned} \gamma &= \frac{T^2(N+m)(N-2m+2)}{2\xi^2 - 2\xi\sqrt{T^2(N+2m)(N-2m+2)+\xi^2} + 2T^2(N+2m)(N-2m+2)}, \\ \eta &= -\frac{T(N+2m)(N-2m+2)\left(\xi - \sqrt{T^2(N+2m)(N-2m+2)+\xi^2}\right)}{4\left(\xi^2 - \xi\sqrt{T^2(N+2m)(N-2m+2)+\xi^2} + T^2(N+2m)(N-2m+2)\right)}. \end{aligned} \tag{12}$$

By diagonalizing $\rho^{(1)}$, one can obtain its two eigenvalues

$$\lambda_{1,2} = \frac{N}{2} \pm \sqrt{(m-\gamma)^2 + \eta^2}. \tag{13}$$

Therefore, F is given as

$$\begin{aligned} F &= \frac{2(N-\lambda_2)}{N} \\ &= \frac{N - 2\sqrt{(m-\gamma)^2+\eta^2}}{N}. \end{aligned} \tag{14}$$

In Fig. 3, we show the dependence of F on δ/E_c. It is clear that the perturbation results (red dashed lines) are well consistent with the numerical results (black lines) for small values of E_J/E_c.

3.2 Entropy

In addition to the Penrose–Onsager condensation criterion, one can characterize the fragmentation via the entropy. On the basis of the concept of the von Neumann entropy, we define the entropy S_1 as

$$S_1 = -\sum_i p_i \ln p_i, \tag{15}$$

where $p_i = \lambda_i/N$ $(i = 1, 2)$ represents the normalized eigenvalues of $\rho^{(1)}$ [67]. We refer to it as the "single body entropy", as it is based on the single-body density matrix. Obviously, we have $p_1 + p_2 = 1$. The entropy S_1 has a maximum of $\ln 2$ when $p_1 = p_2 = 1/2$ and a minimum of 0 when $p_i = \delta_{i,2}$. Therefore, the maximum corresponds to the equal occupation of the two modes, where the ground state is a fully fragmented state, and the minimum corresponds to a single condensate. A nonzero S_1 indicates the existence of fragmentation. This means that S_1 can serve as an alternative quantity to depict the fragmentation.

To characterize the spread of a state in the Fock basis [68], we introduce another entropy S_2, referred to as the "many-body entropy", and

$$S_2 = -\sum_m |C_m|^2 \ln |C_m|^2, \tag{16}$$

where C_m is the probability amplitude. S_2 has a maximum for the equally populated state with $|C_m|^2 = 1/(N+1)$ and a minimum for a macroscopically occupied state with $C_m = \delta_{m;m'}$. As S_1 characterizes the degree of fragmentation, S_2 can be used to study the degree of complexity of a state and to identify whether a many-body quantum state is a single Fock state or a superposition of multiple Fock states.

In Fig. 4, we show S_1 and S_2 versus δ/E_c. Obviously, the dependence of S_1 on δ/E_c is similar to that for F. When $|\delta/E_c|$ decreases, the population difference between the two wells decreases; thus, S_1 increases. Assuming that the tunneling strength can be ignored, a series of steps and notches appear in S_1 owing to the occurrence of single-atom tunneling and the interaction blockade. As the ground state of the system of strong repulsive interactions is a single Fock state with a well-defined number of atoms in each well, we have $S_2 = 0$ between two neighboring critical points. It is also clearly shown that sharp peaks in S_2 appear at the critical points where single-atom tunneling takes place. When the tunneling energy E_J increases, the valleys of S_2 are increased, and the peaks of S_2 are broadened.

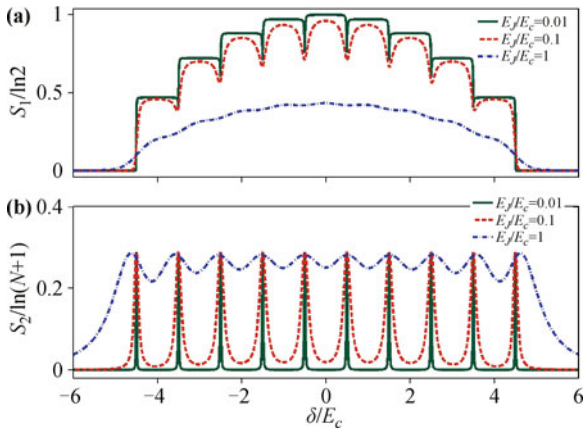

Fig. 4 Ground-state entropies S_1 **(a)** and S_2 **(b)** versus the scaled asymmetry δ/E_c for $E_J/E_c = 1$ (*blue dash-dotted lines*), $E_J/E_c = 0.1$ (*red dashed lines*), and $E_J/E_c = 0.01$ (*green solid lines*). Here, the total number of atoms is $N = 10$.

4 Fragmentation in quantum quenches

In this section, we analyze the dynamic fragmentation in three typical types of asymmetry quenches: linear, sudden, and periodic quenches.

4.1 Linear quench

We consider the linear quench following $\delta(t) = \delta_i + \alpha t$, where α is the sweep rate, and the initial asymmetry $\delta(0) = |\delta_i| \gg E_c$. Apparently, the system possesses no fragmentation for such an initial asymmetry. To obtain a quantitative picture of how the dynamic fragmentation depends on the sweep rate, we calculate the fidelity between the instantaneous state and the instantaneous ground state:

$$P(t) = |\langle \Psi(t)|\mathrm{GS}(\delta/E_c)\rangle|^2, \tag{17}$$

where $|\Psi(t)\rangle$ and $|\mathrm{GS}(\delta/E_c)\rangle$ are the instantaneous state and instantaneous ground states, respectively.

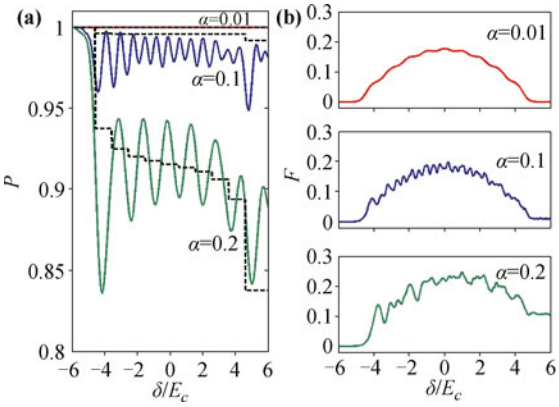

Fig. 5 **(a)** Fidelity P versus δ/E_c for different sweep rates α. The dashed lines are derived from the analytical formula in Eq. (18). **(b)** The degree of fragmentation F versus δ/E_c for different values of α. The other parameters are set as $E_J/E_c = 1$ and $N = 10$.

In Fig. 5, we show F and P for a moderate tunneling strength $E_J/E_c = 1$. For a sufficiently small sweep rate, $\alpha = 0.01$, the system remains in the instantaneous ground state, and F is almost the same as the static one. For a moderate sweep rate, $\alpha = 0.1$, F follows the static one before the system approaches the first LZ transition point. Then, the first LZ tunneling takes place, and F exhibits oscillations. According to LZ theory [69], nonadiabatic transitions take place around an avoided level crossing, and the LZ transition probability is given as $P_{LZ} = \exp(-\frac{\pi\Delta^2}{2\alpha})$, where Δ denotes the minimum energy gap for the avoided crossings. Thus, the probability of finding the system in the instantaneous ground state is $(1 - P_{LZ})$.

By applying the LZ formula to each avoided crossing, the sequential LZ transitions can be regarded as a sequence of two-level LZ transitions. Consequently, the dynamic probabilities of finding the system in the instantaneous ground state after each anticrossing are given as [70]

$$\begin{aligned} &P_1 = 1 - P_{LZ}(\Delta_{01,\alpha}),\\ &P_2 = [1 - P_{LZ}(\Delta_{02,\alpha})][1 - P_{LZ}(\Delta_{01,\alpha})],\\ &\cdots\\ &P_n = \prod_{i=1}^{n}[1 - P_{LZ}(\Delta_{0i,\alpha})]. \end{aligned} \tag{18}$$

In Fig. 5, we show both analytical and numerical results for P. For small sweep rates, the analytical results coincide well with the numerical results.

Owing to the nonadiabatic LZ transitions, the final degree of fragmentation becomes different from the static situation. To reveal the appearance of nonadiabatic transitions, we show the average value of $\hat{J}_z$ for different values of α in Fig. 6(a). Evidently, the final $\langle \hat{J}_z \rangle$ has an increase for large sweep rates, which indicates that the system is no longer a single condensate but a fragmented

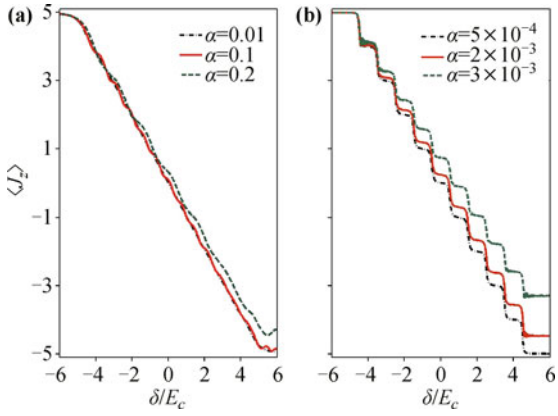

Fig. 6 The average value of J_z versus δ/E_c for **(a)** $E_J/E_c = 1$ and **(b)** $E_J/E_c = 0.1$. Here, the total number of atoms is $N = 10$.

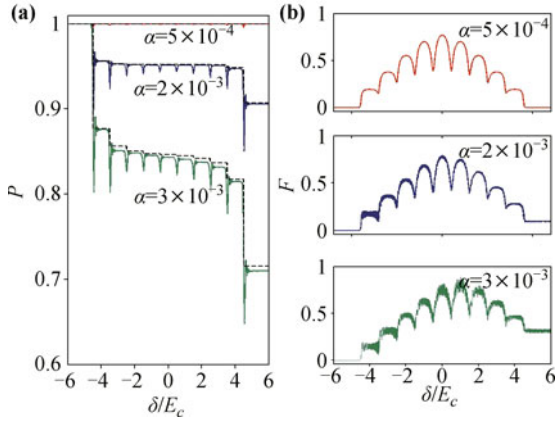

Fig. 7 **(a)** Fidelity P versus δ/E_c for different sweep rates α. The dashed lines correspond to the analytical results given by the sequential LZ picture in Eq. (18). **(b)** The degree of fragmentation F versus δ/E_c for different sweep rates α. The other parameters are set as $E_J/E_c = 0.1$ and $N = 10$.

one. For a larger sweep rate, the fragmentation oscillations are enhanced, and the system ends up with a higher degree of fragmentation.

In Fig. 7, we show F for a weak tunneling strength $E_J/E_c = 0.1$. The degree of fragmentation first remains the same as the static one and then begins to fluctuate when the system approaches the transition points. Similarly, we apply the sequential LZ picture in Eq. (18) to each avoided crossing and find a sharp decrease in the fidelity at the critical points. Owing to the well-defined avoided crossings for weak tunneling, the analytical results given by the sequential LZ picture in Eq. (18) are in very good agreement with the numerical results. Again, the system ends up with a fragmented state for large α.

4.2 Sudden quench

We consider a sudden quench in which the asymmetry is suddenly changed from an initial value to a final value. This can be experimentally achieved by rapidly shifting the center of the confining magnetic trap. We assume that the system is prepared in the ground state $|\Psi(0)\rangle$ of the initial Hamiltonian $\hat{H}_i$ with $\delta = \delta_i$, which corresponds to a fragmented instantaneous ground state. At $t = 0$, δ is suddenly changed to a different value $\delta = \delta_f$, which corresponds to an instantaneous ground state without fragmentation. Then, the system evolves under the final Hamiltonian $\hat{H}_f$.

By using the sudden approximation, the time-evolution is given as [27, 30, 71]

$$|\Psi(t)\rangle = \mathrm{e}^{-\mathrm{i}\hat{H}_f t}\,|\Psi(0)\rangle = \sum_n c_n \mathrm{e}^{-\mathrm{i}E_n t}\,|\psi_n\rangle\,, \tag{19}$$

where E_n and $|\psi_n\rangle$ denote the eigenenergies and eigen-

states of the final Hamiltonian $\hat{H}_f$, respectively. Here, $c_n = \langle\psi_n|\Psi(0)\rangle$ is the overlap between the initial state $|\Psi(0)\rangle$ and the eigenstate $|\psi_n\rangle$. Thus, the time-dependent expectation values of an arbitrary operator are given as

$$\langle\Psi(t)|\mathcal{O}|\Psi(t)\rangle = \sum_{n',n} c_{n',n} e^{-i(E_{n'}-E_n)t} \langle\psi_n|\mathcal{O}|\psi_{n'}\rangle . \tag{20}$$

In Fig. 8, we show the dynamic fragmentation for $\delta_i = -4$, $\delta_f = -5$, and different values of E_J/E_c. We find that the fragmentation exhibits persistent fluctuations around some specific averaged values in all cases, and the fluctuations depend on E_J/E_c. For a moderate $E_J/E_c = 1$, the fragmentation exhibits collapses and revivals. The fluctuation amplitudes increase with E_J/E_c. It is also found that the fragmentations oscillate with more than one frequency that depends on the distribution of the initial state in the spectrum of the final Hamiltonian [27]. To understand the dynamic fragmentation, we project the initial state onto the eigenstates of $\hat{H}_f$ in Fig. 8(b). For $E_J/E_c = 1$, the initial state has a finite overlap with many eigenstates such that the fragmentation has strong fluctuations according to Eq. (20). However, for $E_J/E_c = 0.1$ and $E_J/E_c = 0.01$, the initial state has a large overlap with one eigenstate of the final Hamiltonian such that the fragmentation fluctuations are suppressed.

4.3 Periodic quench

We consider a periodic quench in which the asymmetry is periodically modulated in time: $\delta(t) = \mu\sin(\omega t)$, where μ is the modulation amplitude, and ω is the modulation frequency [70, 72, 73]. The Hamiltonian is as follows:

$$\hat{H}(t) = \hat{H}_0(t) + \hat{H}_1, \tag{21}$$

where the diagonal term is

$$\hat{H}_0(t) = \mu\sin(\omega t)\hat{J}_z + \frac{E_c}{2}\hat{J}_z^2, \tag{22}$$

and the off-diagonal term is

$$\hat{H}_1 = -2T\hat{J}_x. \tag{23}$$

$\hat{H}_0(t)$ is periodic in time; that is, $\hat{H}_0(t) = \hat{H}_0(t+\mathcal{T})$, where $\mathcal{T} = 2\pi/\omega$. According to Floquet's theorem [74, 75], $\hat{H}_0(t)$ has a complete set of solutions in the form of

$$|\Psi_m(t)\rangle = |\Phi_m(t)\rangle\exp(-i\varepsilon_m t/\hbar), \tag{24}$$

where ε_m are the quasienergy, and $|\Phi_m(t)\rangle = \exp\left(i\frac{\mu}{\omega}\cos(\omega t)m\right)|N/2, m\rangle$ is the Floquet function, which is also periodic in time: $|\Phi_m(t)\rangle = |\Phi_m(t+\mathcal{T})\rangle$. Provided ω/T is sufficiently large compared to NE_c/T and there are no significant resonances induced by the periodic driving, one can obtain the effective time-independent Hamiltonian [72, 73]

$$\hat{H} = \frac{E_c}{2}\hat{J}_z^2 - 2T^{\text{eff}}\hat{J}_x. \tag{25}$$

Here, the effective tunneling strength is $T^{\text{eff}} = TJ_0(\frac{2\mu}{\omega})$, where $J_0(x)$ is the zeroth-order Bessel function of the first kind. The renormalization of the tunneling strength facilitates the interplay between the number fluctuations and the phase fluctuations.

In Fig. 9, we show F as a function of the scaled driving amplitude $2\mu/\omega$ for different values of E_J/E_c. It is clearly shown that the periodic driving remarkably modifies F. T^{eff} sensitively relies on $2\mu/\omega$, and it enables the

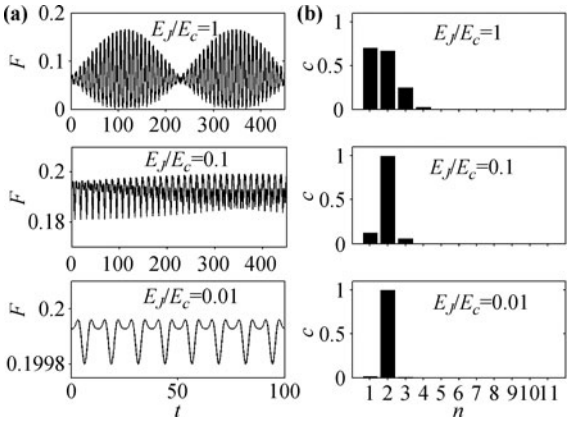

Fig. 8 **(a)** Fragmentation dynamics for different values of E_J/E_c after the quench from $\delta_i = -4$ to $\delta_f = -5$. **(b)** The projection of the initial state onto the spectrum of the final Hamiltonian $\hat{H}(\delta_f)$, corresponding to the left panel. Here, the total number of atoms is $N = 10$.

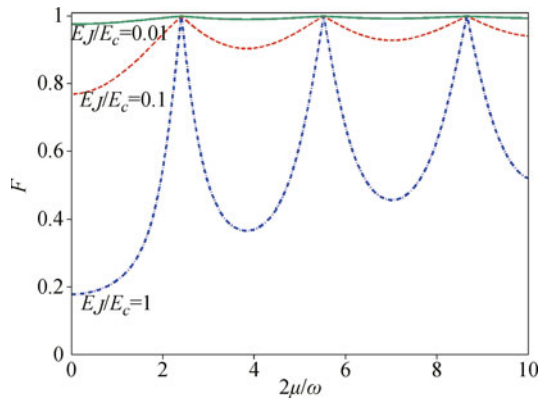

Fig. 9 The fragmentation F versus the scaled driving amplitude $2\mu/\omega$ for $E_J/E_c = 1$ (blue dash-dotted line), $E_J/E_c = 0.1$ (red dashed line), and $E_J/E_c = 0.01$ (green solid line). Here, the total number of atoms is $N = 10$.

possibility of tuning the ratio between the tunneling strength and the interaction strength. Recalling the properties of the zeroth-order Bessel function, $T^{\rm eff}$ quadratically decreases near the zero points of $J_0(x)$, and the tunneling effect is switched off at the zero points of $J_0(x)$, where the system becomes a Fock state with the maximum degree of fragmentation. Each local minimum of F corresponds to a extremum of J_0. The renormalization of the tunneling strength via periodic modulations enables us to tune F.

5 Summary

In summary, we have investigated the fragmentation of a coupled two-mode Bose–Einstein condensate, which undergoes quantum quenches involving LZ transitions. It is found that the interplay between the asymmetry and the interactions may induce a phase transition from a single condensate to a fragmented one. In particular, the appearance of single-atom tunneling and interaction blockades for sufficiently small values of E_J/E_c leads to a series of notches and plateaus in the fragmentation. In further, we consider dynamic fragmentation in three typical kinds of asymmetry quenches. In a linear quench, the final state becomes a fragmented state owing to the sequential LZ processes. A sequence of notches and plateaus appears in the fragmentation, which can be explained by the sequential LZ transitions. We develop a perturbation theory for such a sequential LZ process. In a sudden quench, we find that the fragmentation is more robust for small values of E_J/E_c. In a periodic quench, the fragmentation can be effectively tuned via control of the modulation amplitude and frequency.

Acknowledgements This work was supported by the National Basic Research Program of China under Grant No. 2012CB821305, the National Natural Science Foundation of China under Grant Nos. 11374375 and 11465008, and the Ph.D. Programs Foundation of the Ministry of Education of China under Grant No. 20120171110022.

References

1. O. Penrose and L. Onsager, Bose–Einstein condensation and liquid helium, *Phys. Rev.* 104(3), 576 (1956)
2. A. J. Leggett, Bose–Einstein condensation in the alkali gases: Some fundamental concepts, *Rev. Mod. Phys.* 73(2), 307 (2001)
3. P. Bader and U. R. Fischer, Fragmented many-body ground states for scalar Bosons in a single trap, *Phys. Rev. Lett.* 103(6), 060402 (2009)
4. U. R. Fischer and B. Xiong, Robustness of fragmented condensate many-body states for continuous distribution amplitudes in Fock space, *Phys. Rev. A* 88(5), 053602 (2013)
5. A. I. Streltsov, L. S. Cederbaum, and N. Moiseyev, Ground-state fragmentation of repulsive Bose–Einstein condensates in double-trap potentials, *Phys. Rev. A* 70(5), 053607 (2004)
6. R. Kanamoto, H. Saito, and M. Ueda, Quantum phase transition in one-dimensional Bose–Einstein condensates with attractive interactions, *Phys. Rev. A* 67(1), 013608 (2003)
7. C. J. Myatt, E. A. Burt, R. W. Ghrist, E. A. Cornell, and C. E. Wieman, Production of two overlapping Bose–Einstein condensates by sympathetic cooling, *Phys. Rev. Lett.* 78(4), 586 (1997)
8. D. M. Stamper-Kurn, M. R. Andrews, A. P. Chikkatur, S. Inouye, H. J. Miesner, J. Stenger, and W. Ketterle, Optical confinement of a Bose–Einstein condensate, *Phys. Rev. Lett.* 80(10), 2027 (1998)
9. T. L. Ho and S. K. Yip, Fragmented and single condensate ground states of spin-1 Bose gas, *Phys. Rev. Lett.* 84(18), 4031 (2000)
10. O. E. Müstecaplıoglu, M. Zhang, S. Yi, L. You, and C. P. Sun, Dynamic fragmentation of a spinor Bose–Einstein condensate, *Phys. Rev. A* 68(6), 063616 (2003)
11. A. Görlitz, T. L. Gustavson, A. E. Leanhardt, R. Löw, A. P. Chikkatur, S. Gupta, S. Inouye, D. E. Pritchard, and W. Ketterle, Sodium Bose–Einstein condensates in the in the $F = 2$ state in a large-volume optical trap, *Phys. Rev. Lett.* 90(9), 090401 (2003)
12. H. Schmaljohann, M. Erhard, J. Kronjäger, M. Kottke, S. van Staa, L. Cacciapuoti, J. J. Arlt, K. Bongs, and K. Sengstock, Dynamics of $F = 2$ spinor Bose–Einstein condensates, *Phys. Rev. Lett.* 92(4), 040402 (2004)
13. T. Kuwamoto, K. Araki, T. Eno, and T. Hirano, Magnetic field dependence of the dynamics of ^{87}Rb spin-2 Bose–Einstein condensates, *Phys. Rev. A* 69(6), 063604 (2004)
14. S. Levy, E. Lahoud, I. Shomroni, and J. Steinhauer, The a.c. and d.c. Josephson effects in a Bose–Einstein condensate, *Nature* 449(7162), 579 (2007)
15. R. W. Spekkens and J. E. Sipe, Spatial fragmentation of a Bose–Einstein condensate in a double-well potential, *Phys. Rev. A* 59(5), 3868 (1999)
16. L. Cederbaum and A. Streltsov, Best mean-field for condensates, *Phys. Lett. A* 318(6), 564 (2003)
17. E. J. Mueller, T. L. Ho, M. Ueda, and G. Baym, Fragmentation of Bose–Einstein condensates, *Phys. Rev. A* 74(3), 033612 (2006)
18. T. L. Ho and C. Ciobanu, The Schrödinger cat family in attractive Bose gases, *J. Low Temp. Phys.* 135(3–4), 257 (2004)

19. Q. Zhu, Q. Zhang, and B. Wu, Extended two-site Bose–Hubbard model with pair tunneling: Spontaneous symmetry breaking, effective ground state and fragmentation, *J. Phys. At. Mol. Opt. Phys.* 48(4), 045301 (2015)
20. K. Sakmann, A. I. Streltsov, O. E. Alon, and L. S. Cederbaum, Universality of fragmentation in the Schrödinger dynamics of bosonic Josephson junctions, *Phys. Rev. A* 89(2), 023602 (2014)
21. L. E. Sadler, J. M. Higbie, S. R. Leslie, M. Vengalattore, and D. M. Stamper-Kurn, Spontaneous symmetry breaking in a quenched ferromagnetic spinor Bose–Einstein condensate, *Nature* 443(7109), 312 (2006)
22. S. Hofferberth, I. Lesanovsky, B. Fischer, T. Schumm, and J. Schmiedmayer, Non-equilibrium coherence dynamics in one-dimensional Bose gases, *Nature* 449(7160), 324 (2007)
23. Y. A. Chen, S. D. Huber, S. Trotzky, I. Bloch, and E. Altman, Many-body Landau–Zener dynamics in coupled one-dimensional Bose liquids, *Nat. Phys.* 7(1), 61 (2011)
24. D. Chen, M. White, C. Borries, and B. DeMarco, Quantum quench of an atomic Mott insulator, *Phys. Rev. Lett.* 106(23), 235304 (2011)
25. F. Meinert, M. J. Mark, E. Kirilov, K. Lauber, P. Weinmann, M. Grobner, A. J. Daley, and H. C. Nägerl, Observation of many-body dynamics in long-range tunneling after a quantum quench, *Science* 344(6189), 1259 (2014)
26. C. Lee, W. Hai, L. Shi, X. Zhu, and K. Gao, Chaotic and frequency-locked atomic population oscillations between two coupled Bose–Einstein condensates, *Phys. Rev. A* 64(5), 053604 (2001)
27. K. Sengupta, S. Powell, and S. Sachdev, Quench dynamics across quantum critical points, *Phys. Rev. A* 69(5), 053616 (2004)
28. P. Calabrese and J. Cardy, Time dependence of correlation functions following a quantum quench, *Phys. Rev. Lett.* 96(13), 136801 (2006)
29. C. Kollath, A. M. Läuchli, and E. Altman, Quench dynamics and nonequilibrium phase diagram of the Bose–Hubbard model, *Phys. Rev. Lett.* 98(18), 180601 (2007)
30. G. Roux, Quenches in quantum many-body systems: One-dimensional Bose–Hubbard model reexamined, *Phys. Rev. A* 79(2), 021608 (2009)
31. B. Sciolla and G. Biroli, Quantum quenches and off-equilibrium dynamical transition in the infinite-dimensional Bose–Hubbard model, *Phys. Rev. Lett.* 105(22), 220401 (2010)
32. J. Dziarmaga and M. Tylutki, Excitation energy after a smooth quench in a Luttinger liquid, *Phys. Rev. B* 84(21), 214522 (2011)
33. D. Poletti and C. Kollath, Slow quench dynamics of periodically driven quantum gases, *Phys. Rev. A* 84(1), 013615 (2011)
34. F. H. L. Essler, S. Evangelisti, and M. Fagotti, Dynamical correlations after a quantum quench, *Phys. Rev. Lett.* 109(24), 247206 (2012)
35. X. Yin and L. Radzihovsky, Quench dynamics of a strongly interacting resonant Bose gas, *Phys. Rev. A* 88(6), 063611 (2013)
36. J. S. Bernier, R. Citro, C. Kollath, and E. Orignac, Correlation dynamics during a slow interaction quench in a one-dimensional Bose gas, *Phys. Rev. Lett.* 112(6), 065301 (2014)
37. E. J. Torres-Herrera and L. F. Santos, Quench dynamics of isolated many-body quantum systems, *Phys. Rev. A* 89(4), 043620 (2014)
38. M. Eckstein, M. Kollar, and P. Werner, Thermalization after an interaction quench in the Hubbard model, *Phys. Rev. Lett.* 103(5), 056403 (2009)
39. M. Rigol, Breakdown of thermalization in finite one-dimensional systems, *Phys. Rev. Lett.* 103(10), 100403 (2009)
40. M. Cazalilla and M. Rigol, Focus on dynamics and thermalization in isolated quantum many-body systems, *New J. Phys.* 12(5), 055006 (2010)
41. A. Polkovnikov, K. Sengupta, A. Silva, and M. Vengalattore, Colloquium: Nonequilibrium dynamics of closed interacting quantum systems, *Rev. Mod. Phys.* 83(3), 863 (2011)
42. A. C. Cassidy, C. W. Clark, and M. Rigol, Generalized thermalization in an integrable lattice system, *Phys. Rev. Lett.* 106(14), 140405 (2011)
43. C. A. Parra-Murillo, J. Madroñero, and S. Wimberger, Quantum diffusion and thermalization at resonant tunneling, *Phys. Rev. A* 89(5), 053610 (2014)
44. W. H. Zurek, U. Dorner, and P. Zoller, Dynamics of a quantum phase transition, *Phys. Rev. Lett.* 95(10), 105701 (2005)
45. C. Lee, Universality and anomalous mean-field breakdown of symmetry-breaking transitions in a coupled two-component Bose–Einstein condensate, *Phys. Rev. Lett.* 102(7), 070401 (2009)
46. J. Dziarmaga and M. M. Rams, Dynamics of an inhomogeneous quantum phase transition, *New J. Phys.* 12(5), 055007 (2010)
47. J. Dziarmaga, M. Tylutki, and W. H. Zurek, Quench from Mott insulator to superfluid, *Phys. Rev. B* 86(14), 144521 (2012)
48. F. Meinert, M. J. Mark, E. Kirilov, K. Lauber, P. Weinmann, A. J. Daley, and H. C. Nägerl, Quantum quench in an atomic one-dimensional Ising chain, *Phys. Rev. Lett.* 111(5), 053003 (2013)
49. U. Schneider, L. Hackermuller, J. P. Ronzheimer, S. Will, S. Braun, T. Best, I. Bloch, E. Demler, S. Mandt, D. Rasch, and A. Rosch, Fermionic transport and out-of-equilibrium dynamics in a homogeneous Hubbard model with ultracold atoms, *Nat. Phys.* 8(3), 213 (2012)
50. M. Cheneau, P. Barmettler, D. Poletti, M. Endres, P. Schausz, T. Fukuhara, C. Gross, I. Bloch, C. Kollath, and S. Kuhr, Light-cone-like spreading of correlations in a quantum many-body system, *Nature* 481(7382), 484 (2012)

51. J. P. Ronzheimer, M. Schreiber, S. Braun, S. S. Hodgman, S. Langer, I. P. McCulloch, F. Heidrich-Meisner, I. Bloch, and U. Schneider, Expansion dynamics of interacting Bosons in homogeneous lattices in one and two dimensions, *Phys. Rev. Lett.* 110(20), 205301 (2013)
52. P. Jurcevic, B. P. Lanyon, P. Hauke, C. Hempel, P. Zoller, R. Blatt, and C. F. Roos, Quasiparticle engineering and entanglement propagation in a quantum many-body system, *Nature* 511(7508), 202 (2014)
53. G. J. Milburn, J. Corney, E. M. Wright, and D. F. Walls, Quantum dynamics of an atomic Bose–Einstein condensate in a double-well potential, *Phys. Rev. A* 55(6), 4318 (1997)
54. X. X. Yang and Y. Wu, $SU(2)$ coherent state description of two-mode Bose–Einstein condensates, *Commum. Theor. Phys.* 37(5), 539 (2002)
55. L. M. Kuang, J. H. Li, and B. Hu, Polarization and decoherence in a two-component Bose–Einstein condensate, *J. Opt. B* 4(5), 295 (2002)
56. A. H. Zeng and L. M. Kuang, Influence of quantum entanglement on quantum tunnelling between two atomic Bose–Einstein condensates, *Phys. Lett. A* 338(3–5), 323 (2005)
57. C. Lee, Adiabatic Mach–Zehnder interferometry on a quantized Bose–Josephson junction, *Phys. Rev. Lett.* 97(15), 150402 (2006)
58. D. Witthaut, F. Trimborn, and S. Wimberger, Dissipation induced coherence of a two-mode Bose–Einstein condensate, *Phys. Rev. Lett.* 101(20), 200402 (2008)
59. X. X. Yang and Y. Wu, Effective two-state model and NOON states for double-well Bose–Einstein condensates in strong-interaction regime, *Commum. Theor. Phys.* 52(2), 244 (2009)
60. F. Trimborn, D. Witthaut, V. Kegel, and H. Korsch, Nonlinear Landau–Zener tunneling in quantum phase space, *New J. Phys.* 12(5), 053010 (2010)
61. C. Lee, J. Huang, H. Deng, H. Dai, and J. Xu, Nonlinear quantum interferometry with Bose condensed atoms, *Front. Phys.* 7(1), 109 (2012)
62. S. S. Li, J. B. Yuan, and L. M. Kuang, Coherent manipulation of spin squeezing in atomic Bose–Einstein condensate via electromagnetically induced transparency, *Front. Phys.* 8(1), 27 (2013)
63. A. Sinatra, J. C. Dornstetter, and Y. Castin, Spin squeezing in Bose–Einstein condensates: Limits imposed by decoherence and non-zero temperature, *Front. Phys.* 7(1), 86 (2012)
64. R. Gati and M. K. Oberthaler, A bosonic Josephson junction, *J. Phys. At. Mol. Opt. Phys.* 40(10), R61 (2007)
65. W. D. Li, Y. Zhang, and J. Q. Liang, Energy-band structure and intrinsic coherent properties in two weakly linked Bose–Einstein condensates, *Phys. Rev. A* 67(6), 065601 (2003)
66. C. Lee, L. B. Fu, and Y. S. Kivshar, Many-body quantum coherence and interaction blockade in Josephson-linked Bose–Einstein condensates, *Europhys. Lett.* 81(6), 60006 (2008)
67. D. Raventós, T. Graß, and B. Juliá-Díaz, Cold bosons in optical lattices: Correlations, localization, and fragmentation, arXiv: 1410.7280
68. B. Juli'a-Diaz, D. Dagnino, M. Lewenstein, J. Martorell, and A. Polls, Macroscopic self-trapping in Bose–Einstein condensates: Analysis of a dynamical quantum phase transition, *Phys. Rev. A* 81(2), 023615 (2010)
69. C. Zener, Non-Adiabatic crossing of energy levels, *Proceedings of the Royal Society of London Series A* 137, 696 (1932)
70. H. Zhong, Q. Xie, J. Huang, X. Qin, H. Deng, J. Xu, and C. Lee, Photon-induced sideband transitions in a many body Landau–Zener process, *Phys. Rev. A* 90(2), 023635 (2014)
71. E. J. Torres-Herrera and L. F. Santos, Non-exponential fidelity decay in isolated interacting quantum systems, *Phys. Rev. A* 90(3), 033623 (2014)
72. A. Eckardt, T. Jinasundera, C. Weiss, and M. Holthaus, Analog of photon-assisted tunneling in a Bose–Einstein condensate, *Phys. Rev. Lett.* 95(20), 200401 (2005)
73. T. Jinasundera, C. Weiss, and M. Holthaus, Manyparticle tunnelling in a driven Bosonic Josephson junction, *Chem. Phys.* 322(1–2), 118 (2006)
74. M. Grifoni and P. Hänggi, Driven quantum tunneling, *Phys. Rep.* 304(5–6), 229 (1998)
75. G. Liu, N. Hao, S. L. Zhu, and W. M. Liu, Topological superfluid transition induced by a periodically driven optical lattice, *Phys. Rev. A* 86(1), 013639 (2012)